

APLA: A Simple Adaptation Method for Vision Transformers

Moein Sorkhei^{1,2 *} Emir Konuk^{1,2} Kevin Smith^{1,2 †} Christos Matsoukas^{1,2 †}

¹ KTH Royal Institute of Technology, Stockholm, Sweden

²Science for Life Laboratory, Stockholm, Sweden

Abstract

Existing adaptation techniques typically require architectural modifications or added parameters, leading to high computational costs and complexity. We introduce Attention Projection Layer Adaptation (APLA), a simple approach to adapt vision transformers (ViTs) without altering the architecture or adding parameters. Through a systematic analysis, we find that the layer immediately after the attention mechanism is crucial for adaptation. By updating only this projection layer, or even just a random subset of this layer’s weights, APLA achieves state-of-the-art performance while reducing GPU memory usage by up to 52.63% and training time by up to 43.0%, with no extra cost at inference. Across 46 datasets covering a variety of tasks including scene classification, medical imaging, satellite imaging, and fine-grained classification, APLA consistently outperforms 17 other leading adaptation methods, including full fine-tuning, on classification, segmentation, and detection tasks. The code is available at github.com/MoeinSorkhei/APLA.

1. Introduction

The primary objective of model adaptation is to enable models to generalize to new tasks with minimal data and computational cost. The most successful approaches accomplish this by injecting new parameters or layers into frozen foundation models [6, 29, 31, 42]. This process often requires complex heuristics – such as gradient sensitivity analyses [23, 69] and neural architecture searches [68]—to determine the optimal locations to inject parameters. Furthermore, the addition of new parameters can introduce significant overhead. Aiming at better efficiency, a handful of methods attempt to adapt the existing structure of the model without adding parameters [66, 69], but these methods underperform compared to parameter-adding techniques. This raises a critical question: is it possible to achieve competitive adaptation using only a model’s existing architecture?

*Corresponding author: Moein Sorkhei <sorkhei@kth.se>

†Equal contribution.

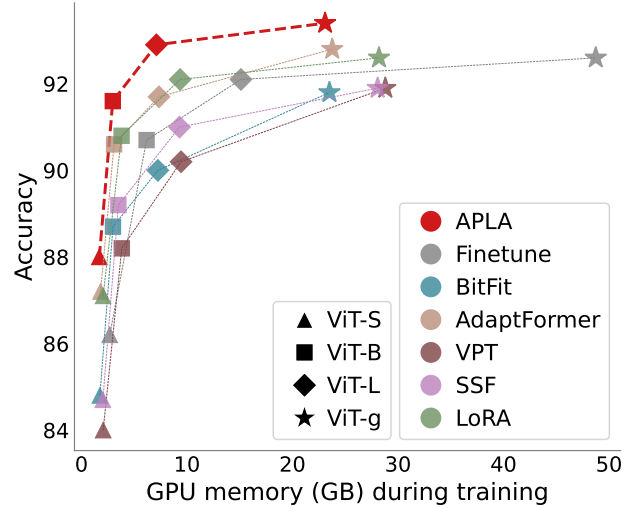


Figure 1. APLA achieves state-of-the-art for ViT adaption. It yields better performance for a given GPU memory budget during training compared to full fine-tuning and leading adaptation methods. Similar savings are observed at inference (see Appendix B).

We propose that the answer is *yes* – and that the key is to better leverage the model’s inherent architecture.

We systematically investigate which existing components of a Vision Transformer (ViT) foundation model are most essential for adaptation in a departure from traditional parameter-adding approaches. Our analysis reveals that the projection layer immediately following the multi-head self-attention (MSA) mechanism plays a uniquely critical role. Then, inspired by low-rank approximation techniques [29, 32], which demonstrate that updates to a full weight matrix can often be effectively represented with lower-dimensional matrices, we explore whether updating the entire projection layer is necessary. We find that *modifying only a random subset of this layer’s parameters* is sufficient to maintain – or even surpass – performance, while further reducing computational costs. This result suggests that additional parameters used to learn a low-rank approximation of the updates may be unnecessary, opening the door for simpler, more efficient adaptation strategies.

In this work, we introduce Attention Projection Layer

Adaptation (APLA), a novel state-of-the-art approach for efficient adaptation of ViTs that requires no additional parameters. Our key contributions are as follows:

- **Identification of a critical ViT component:** Through systematic experimentation, we identify the projection layer immediately following the attention mechanism as the most essential component for adaptation, offering a targeted approach to ViT tuning essential to APLA which can also improve other adaptation techniques.
- **Low-rank subset update for efficient adaptation:** Building on this insight, we introduce a low-rank adaptation technique that updates only a *random subset* of the projection layer’s weights, achieving higher performance with even lower computational costs.
- **Simplified adaptation with no extra parameters:** Our method achieves SOTA results without introducing any new parameters, and eliminates the need for costly heuristics to determine where to inject new parameters or adapt existing ones.
- **Validated across scales and diverse applications:** We validate APLA on 46 datasets across various tasks and model sizes, demonstrating its consistent superiority over 17 adaptation methods. *In most cases, APLA performs better than full fine-tuning* while also achieving up to 52.63% in GPU memory savings and a 43.0% reduction in training time.

Together, these contributions establish APLA as a new standard for efficient and accessible ViT adaptation.

2. Related Work

Foundation models [3] have transformed computer vision, but as these models grow larger [14, 30, 51], their fine-tuning requires high memory and computational resources. The traditional *pretrain, then fine-tune* paradigm [12, 44, 49, 70] has driven the field for years, but is becoming unfeasible for many applications due to these increasing costs. Recent advancements in model size [14, 30, 51] have only increased these challenges, making full fine-tuning unfeasible for many applications.

In response, efficient adaptation methods have emerged, allowing practitioners with fewer resources to leverage large foundation models by introducing only a small set of new parameters, often called parameter-efficient fine-tuning (PEFT). These methods reduce overhead, making large models more deployable in limited-resource settings.

Adapter-based methods introduce compact, lightweight modules into specific layers, enabling task-specific adaptation by tuning only the adapter parameters while keeping the base model largely frozen. Originally developed for NLP, Adapters [28] place bottleneck modules sequentially after each multi-head attention and MLP block [61]. AdaptFormer [6] extends this for vision transformers, placing adapters in parallel with the MLP blocks rather than se-

quentially. More recent methods refine adapter designs for greater efficiency. ARC [16] uses a similar bottleneck operation but introduces parameter-sharing. SPT-Adapter [23] identifies and adapts only the most impactful layers based on gradient magnitudes. SSF [42] appends learnable scaling and shifting transformations to modulate features after each ViT layer, while Consolidator [22] adds grouped connected layers that capture richer information through channel-wise input groups. Adapter-based methods provide flexible, efficient model adaptation with fewer parameters than full fine-tuning. However, they increase inference costs, require careful initialization [28, 56], and their placement often relies on heuristics [6] or gradient-based selection [23], adding computational overhead and potentially leading to suboptimal configurations.

Low-rank-based methods leverage the low-rank structure in adaptation updates, enabling efficient adaptation through low-rank matrices. LoRA [29] pioneered this approach by adding low-rank matrices alongside original weights in attention blocks. SPT-LoRA [23] builds on LoRA by selectively applying low-rank updates to layers with the largest gradient magnitudes. FacT [32] and RLRR [17] decompose updates into factors, applying these across all ViT layers. While low-rank methods reduce adaptation costs, they insert additional parameters similarly to adapters.

Prompt-based methods introduce learnable tokens to guide adaptation without modifying core model parameters. VPT [31] adds tokens to the input of each transformer block, and E²VPT [21] incorporates auxiliary tokens into attention layers as well. Though prompt-based methods avoid changing internal parameters, they can increase inference costs due to the added tokens. NOAH [68] combines prompts with adapters and LoRA modules, using neural architecture search to optimize placement.

Parameter-selective tuning is an approach used by a handful of methods most closely related to APLA, that focus on adapting models by tuning only a subset of their existing parameters. GPS [69] selects parameters for tuning based on their gradient magnitudes, targeting the most error-inducing parameters during adaptation. BitFit [66] takes a simpler approach, updating only the bias parameters. While these methods can be computationally efficient and easy to implement, they face challenges in identifying an optimal subset of parameters, which is reflected in their comparatively poor performance. APLA addresses this by identifying and targeting a critical layer for adaptation in ViTs, achieving state-of-the-art performance.

3. Methods

Inspired by methods that tune a subset of network weights and approaches that use low-rank updates, we ask, “*Can we combine the strengths of both?*” To this end, we identify the most impactful ViT components for adaptation and propose

a simple method that updates a low-rank subset of existing weights.

3.1. Investigating adaptability of ViT components

A ViT is composed of multiple learnable components. To identify the most impactful ones for adapting the model to downstream tasks, we first review the different ViT components, grouped by their function (Figure 2).

Starting with an input image x , a patchifying stem tiles and reshapes it into N flattened patches. Each patch undergoes a linear transformation in the embedding layer W_E with positional embeddings $\text{Pos}_n, n \in \{1, \dots, N\}$ added to capture spatial information and a classification token [CLS] appended to create the initial embeddings z_0 . These embeddings are passed through L transformer blocks, each containing LayerScale (LS) [57], LayerNorm (LN) [1], multi-head self-attention (MSA), and multi-layer perceptron (MLP) modules. The final representation is typically derived from the [CLS] token of the L th block, which is then processed by classification head W_{pred} to produce the prediction \hat{y} .

In the MSA block, self-attention is computed for the input tokens using the learnable matrices W_{Q_i}, W_{K_i} , and W_{V_i} , where $i \in \{1, \dots, h\}$ corresponds to h parallel self-attention heads, allowing each head to learn distinct contextual relationships. The self-attention output for each head is given by:

$$\text{head}_i = \text{softmax} \left(\frac{(z_{in} W_{Q_i})(z_{in} W_{K_i})^T}{\sqrt{d_h}} \right) (z_{in} W_{V_i}) \quad (1)$$

where d_h is the dimensionality of the Query, Key, and Value vectors for each self-attention head. The outputs from each head_i are concatenated, and a projection layer W_O reweights the combined features to form the final output of the MSA block.

$$z_{out} = [\text{head}_1; \text{head}_2; \dots; \text{head}_h] W_O \quad (2)$$

This output is then processed by an MLP block, consisting of two fully connected layers, W_{FC_1} and W_{FC_2} , with a non-linearity in between.

To identify the most essential component for adaptation, we conducted an empirical investigation by selectively tuning each of the components described above, one at a time (Figure 2) along with the final classification head W_{pred} , while keeping the rest of the network frozen. We found that tuning only the projection layer W_O —positioned directly after the self-attention operation in the MSA block—yields the best performance, even surpassing full fine-tuning. Details of this study are provided in Section 5.1.

3.2. Low-rank adaptation through partial gradients

Low-rank adaptation methods leverage the insight that the difference between initial and adapted values of a full-rank

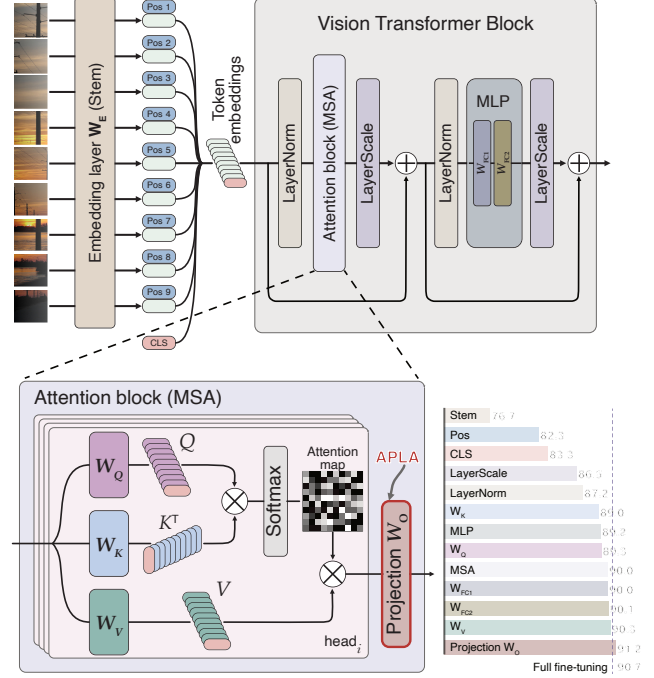


Figure 2. Investigating adaptation performance of individual ViT components. We evaluate the adaptation effectiveness of each ViT component in isolation across various downstream tasks, reporting the average performance. Results show that the attention output projection layer (W_O), located immediately after the attention mechanism, is the most effective for adaptation. See Section 5.1 and Table 1 for detailed results.

matrix can be closely approximated by a low-rank matrix

$$W_{\text{approx}} \approx W_{\text{final}} - W_{\text{init}}, \quad \text{rank}(W_{\text{approx}}) \leq d$$

where W_{init} and W_{final} are the layer’s learnable matrix before and after adaptation, and d is the full rank. Prior works (e.g. [29, 32]) approximate this difference by adding low-rank matrices to ViT layers, with the rank $r := \text{rank}(W_{\text{approx}})$ set as a hyperparameter.

In contrast, we propose a simpler low-rank adaptation by computing gradients on a *randomly selected* subset of columns, which achieves substantial computational savings and retains the benefits of low-rank updates without adding parameters or altering the model’s architecture.

Specifically, given a parameter matrix $W \in \mathbb{R}^{d \times d}$, we partition it into a trainable sub-matrix $W_t \in \mathbb{R}^{d \times r}$ where gradients are computed during training, and a frozen sub-matrix $W_f \in \mathbb{R}^{d \times (d-r)}$, which remains unchanged.

$$W_t = W[i, j_m] \quad m = 1, 2, \dots, r \quad (3)$$

where the brackets denote indexing with $\{j_1, j_2, \dots, j_r\} \subseteq \{1, 2, \dots, d\}$, representing randomly selected trainable column indices, where r controls the rank of the update, reaching full rank when $r = d$.

Table 1. *The importance of ViT components for adaptation.* We evaluate how tuning each ViT component in isolation affects performance, while keeping the rest of the model frozen. We report classification performance, with the **best** and **second best** results highlighted; this notation is used in subsequent tables.

	Birds	Cars	AID	ISIC	Average
[CLS] token	83.9	89.9	92.9	66.4	83.3
positional embeddings	85.1	89.6	92.9	61.4	82.3
Embedding layer W_E	85.7	88.2	87.9	45.1	76.7
LayerNorm	83.7	91.5	94.6	79.0	87.2
LayerScale	85.5	91.2	93.9	75.4	86.5
W_Q weight matrix	85.5	91.8	94.6	85.1	89.3
W_K weight matrix	85.8	91.8	94.5	83.8	89.0
W_V weight matrix	85.8	93.2	95.3	86.9	90.3
W_O weight matrix	86.5	94.0	96.0	88.2	91.2
MSA block	85.0	93.8	94.7	86.5	90.0
W_{FC1} weight matrix	84.7	93.5	95.0	86.9	90.0
W_{FC2} weight matrix	84.6	93.4	94.7	87.7	90.1
MLP block	82.4	93.6	94.3	86.4	89.2
Full Finetuning	<u>85.2</u>	94.4	<u>95.4</u>	<u>87.7</u>	<u>90.7</u>

3.3. Attention Projection Layer Adaptation (APLA)

Foundation models already encode a rich set of features, and we hypothesize that adapting to new tasks can be achieved by selectively re-weighting these features to fit the target task. Therefore, our approach to efficient model adaptation focuses on identifying impactful layers and computing partial gradients on a randomly selected subset of output features (matrix columns).

The projection layer W_O is an ideal target for adaptation as it plays a central role in re-weighting features from the attention mechanism across all the heads.

Therefore, we propose *Attention Projection Layer Adaptation* (APLA), which tunes a randomly selected subset of columns in the W_O^l matrices in each transformer block, while keeping the rest of the ViT backbone frozen. Specifically, we tune only a subset of column vectors of the W_O^l matrices and the final classification head W_{pred} :

$$\mathcal{S}_{\text{APLA}} = \{W_O^1[i, j_m^1], W_O^2[i, j_m^2], \dots, W_O^L[i, j_m^L], W_{\text{pred}}\} \quad (4)$$

For each transformer block $l \leq L$, we independently sample a distinct subset of column indices $\{j_1^l, j_2^l, \dots, j_r^l\} \subseteq \{1, 2, \dots, d\}$ given a global rank hyperparameter $r \leq d$, chosen once at the beginning of training.

APLA is easy to implement, computationally efficient, requires no new parameters, and introduces no additional inference latency, making it highly practical.

4. Experimental Setup

We benchmark APLA against 21 adaptation methods on 46 datasets across 4 tasks, using 3 foundation models. For our main model types, we use Vision Transformers (ViTs) [18] and Swin Transformers [44] at varying capacities, unless stated otherwise. Below, we provide an overview of our

Table 2. *Comparing parameter-selection strategies for APLA.*

	NABirds	SUN397	Cal-256	Cal-101	Oxf-Pet	DDSM	Average
Largest gradients	88.1	78.3	95.3	97.4	95.9	97.2	92.0
Largest activations	87.8	<u>78.5</u>	<u>95.6</u>	97.7	96.1	96.7	<u>92.1</u>
Largest weight magnitude	87.8	78.6	95.5	97.8	<u>96.0</u>	97.0	<u>92.1</u>
Random (APLA)	<u>88.0</u>	78.3	95.7	98.0	96.1	97.2	92.2

experimental setup. Additional details are available in Appendix A.

Adaptation methods We evaluate APLA against various adaptation methods, beginning with traditional approaches: full fine-tuning (FINETUNE) and training only an appended linear layer (LINEAR). We further compare against MLP- k and PARTIAL- k . In MLP- k , a k -layer MLP is appended to the model, and only this block is trained, while PARTIAL- k tunes the last k blocks of the model. We set $k = 3$ for MLP- k and $k = 1$ for PARTIAL- k , in line with [31]. To benchmark efficient adaptation, we compare against 17 recent methods: BITFIT [66], ADAPTER [28], ADAPT-FORMER [6], VPT-shallow and VPT-deep [31], E²VPT [21], SSF [42], LORA [29], SPT-adapter and SPT-LoRA [23], NOAH [68], FACT-TK and FACT-TT [32], CONSOLIDATOR [22] ARC [16], GPS [69] and RLRR [17].

Datasets and tasks We benchmark APLA across 46 datasets, covering a diverse set of object categories and tasks. Starting with 21 generic image classification tasks, we cover superordinate object recognition, fine-grained classification, scene recognition, satellite imagery, and medical image analysis using the following datasets: CUB-200-2011 [62], NABirds [60], Birdsnap [2], Stanford Dogs [36], StanfordCars [39], Aircraft [46], Caltech-256 [20], Caltech-101 [19], CIFAR-100 and CIFAR-10 [40], Oxford-III Pet [52], DTD [8], MIT Indoor [54], SUN397 [64], AID [63], RSSCN7 [7], ISIC2019 [9, 10, 58], APTOS2019 [33], DDSM [41], Colorectal [34], and Pneumonia [35].

For semantic & instance segmentation and object detection we use ADE20K [71, 72] and MS COCO [43].

To test in low-data settings, we use VTAB-1k [67], a collection of 19 classification tasks with only 1,000 training examples each—representing challenging yet realistic scenarios for model adaptation. For out-of-distribution (OOD) evaluation, we use ImageNet, ImageNet-A [27], ImageNet-C [25], and ImageNet-R [26], which introduce various domain shifts, including corruptions, perturbations, and adversarial examples. We use the standard evaluation metric for each dataset.

Foundation models To assess the impact of the foundation model type and pretraining strategy, we compare models trained on IMAGENET-21K [15] using supervised learning, OPENCLIP [30] trained with semi-supervision, and

Table 3. *Main results comparing adaptation methods on image classification for ViT-B [18] pre-trained with DINOv2 [51]. The best and second best results are highlighted for each task.*

	Fine-grained							General							Scene			Satellite			Medical						
	CUB-200-2011	NA Birds	Birdsnap	StanfordDogs	StanfordCars	Aircraft	Average	Caltech-256	Caltech-101	CIFAR-100	CIFAR-10	Oxford-IIIT Pet	DTD	Average	MIT-Indoor	SUN397	Average	AID	RSSCN7	Average	ISIC2019	APTOS2019	DDSM	Colorectal	Pneumonia	Average	Total Average
FINETUNE	88.9	85.2	78.7	86.0	<u>94.4</u>	87.5	86.8	93.9	97.3	92.4	98.7	94.7	81.9	93.1	87.8	75.6	81.7	95.4	73.3	84.4	<u>87.7</u>	90.8	95.5	97.8	<u>99.4</u>	94.2	89.7
LINEAR	89.1	86.6	79.4	87.6	88.4	76.5	84.6	94.9	97.0	88.9	98.0	95.8	81.1	92.6	88.9	76.4	82.7	91.2	77.1	84.2	55.3	90.4	89.4	94.0	97.9	85.4	86.9
MLP	89.1	86.4	78.9	87.8	88.3	77.7	84.7	94.4	97.5	89.2	98.4	<u>96.0</u>	80.9	92.7	88.6	76.2	82.4	91.6	76.4	84.0	71.9	90.7	93.4	95.8	97.9	89.9	88.0
PARTIAL	88.8	86.5	78.6	87.4	88.1	76.6	84.3	94.9	96.9	89.0	98.0	<u>96.0</u>	80.6	92.6	88.5	76.3	82.4	90.9	77.7	84.3	56.1	90.6	89.5	94.2	97.6	85.6	86.8
BITFit	89.4	87.9	80.7	87.8	92.5	83.2	86.9	95.2	97.6	93.1	99.3	95.7	82.2	93.9	89.3	77.7	83.5	95.2	83.5	89.4	79.0	90.1	96.4	97.2	99.1	92.4	90.1
ADAPTER	<u>89.6</u>	88.4	80.0	87.8	93.5	86.1	<u>87.6</u>	95.0	97.6	<u>93.5</u>	99.3	95.9	81.8	93.9	89.5	77.9	83.7	95.0	84.2	89.6	84.3	89.6	96.1	<u>98.0</u>	98.5	93.3	90.6
ADAPTFORMER	89.7	88.4	80.5	88.1	93.1	85.4	87.5	95.6	98.1	93.2	99.3	95.9	82.8	<u>94.2</u>	89.9	<u>78.1</u>	<u>84.0</u>	95.4	<u>85.3</u>	<u>90.4</u>	85.6	90.8	97.3	97.4	98.6	93.9	90.9
VPT-SHALLOW	88.8	86.7	79.1	87.4	90.6	73.2	84.3	95.1	97.2	92.4	99.1	<u>96.0</u>	80.4	93.4	89.4	76.6	83.0	91.6	70.4	81.0	76.5	89.3	96.2	96.4	98.7	91.4	88.1
VPT-DEEP	89.1	87.3	79.9	87.2	91.5	81.7	86.1	95.3	97.8	92.7	99.1	95.7	80.5	93.5	<u>90.0</u>	77.0	83.5	94.4	78.0	86.2	79.6	91.0	96.2	97.6	98.8	92.6	89.5
E ² VPT	88.3	86.6	79.7	87.4	91.2	81.0	85.7	94.5	96.9	92.7	<u>99.2</u>	95.4	79.6	93.1	88.7	76.3	82.5	93.7	72.7	83.2	80.9	90.6	96.2	96.8	98.6	92.6	88.9
SSF	89.4	<u>88.1</u>	80.5	87.7	92.7	83.7	87.0	95.3	97.8	93.2	<u>99.2</u>	95.7	82.1	93.9	88.9	77.4	83.2	95.3	82.6	89.0	80.7	90.5	96.4	97.2	99.0	92.8	90.2
LoRA	88.7	87.5	79.3	86.3	93.4	86.4	86.9	94.3	97.1	93.0	<u>99.0</u>	94.0	80.4	93.0	88.5	76.4	82.5	95.4	81.4	88.4	86.5	<u>91.1</u>	95.1	97.4	98.9	93.8	90.0
SPT-ADAPTER	89.4	<u>88.1</u>	80.6	87.7	93.1	86.2	87.5	95.8	97.5	93.1	<u>99.2</u>	95.8	82.7	94.0	89.5	<u>78.1</u>	83.8	<u>95.6</u>	84.7	90.2	82.1	90.4	96.1	97.2	99.0	93.0	90.6
SPT-LoRA	89.2	87.9	80.6	87.5	92.8	86.3	87.4	95.8	97.7	92.6	<u>99.2</u>	95.7	82.3	93.9	89.9	77.7	83.8	95.4	84.2	89.8	82.2	89.3	96.2	97.4	99.1	92.8	90.4
FACT-TK	88.8	87.8	80.5	87.5	93.0	85.4	87.2	95.3	97.6	92.8	<u>99.2</u>	95.5	81.5	93.7	88.9	77.4	83.2	95.4	79.9	87.7	85.1	91.5	96.3	97.2	97.9	93.6	90.2
FACT-TT	88.8	87.6	79.7	87.1	92.9	84.3	86.7	94.9	97.5	92.4	<u>99.2</u>	95.5	81.7	93.5	89.4	77.1	83.3	94.5	80.6	87.6	81.5	90.9	97.0	97.4	98.6	93.1	89.9
CONSOLIDATOR	89.7	87.4	<u>81.5</u>	87.1	93.0	83.4	87.0	94.5	97.3	92.7	99.0	95.8	81.8	93.5	89.5	77.0	83.3	94.6	78.0	86.3	81.9	<u>91.1</u>	96.9	96.2	<u>99.4</u>	93.1	89.9
ARC	89.4	88.2	80.7	<u>88.1</u>	<u>92.6</u>	84.1	87.2	95.8	97.8	92.9	<u>99.2</u>	96.0	82.8	94.1	89.8	78.2	84.0	95.6	86.2	90.9	82.5	90.7	97.3	97.0	98.8	93.3	90.7
GPS	89.1	86.4	80.7	86.6	94.7	85.5	87.2	94.8	97.6	94.0	99.3	94.4	77.9	93.0	88.4	76.9	82.7	94.9	61.6	78.3	87.7	90.8	96.7	97.4	99.3	94.4	89.3
RLRR	88.9	87.9	80.8	87.6	92.4	83.7	86.9	95.2	97.4	93.1	<u>99.2</u>	95.8	82.0	93.8	89.5	77.6	83.6	95.0	81.2	88.1	81.7	90.4	96.3	96.6	98.6	92.7	90.0
APLA	<u>89.6</u>	88.0	81.9	88.5	94.0	<u>86.7</u>	88.1	<u>95.7</u>	<u>98.0</u>	93.4	99.3	96.1	83.0	94.3	90.4	78.3	84.4	96.0	86.2	91.1	88.2	92.1	<u>97.2</u>	98.4	99.5	95.1	91.5

DINOv2 [51], pre-trained using self-supervision. We utilize DINOv2 unless stated otherwise.

Implementation details To ensure fair comparison, we closely follow the implementations in [6, 16, 17, 21, 29, 31, 32]. For each dataset, we use the official protocol and standard train/val/test splits when available [67] or the splits provided by [31]. Models are trained with AdamW [45] for 100 epochs, using a cosine decay learning rate schedule with a 10-epoch warm-up. Hyperparameters are selected via grid search on the validation set.

APLA, like other low-rank methods (e.g. [29, 32]), requires selecting the value r , which in our case represents the number of columns of the weight matrix sampled for adaptation. We search over $r \in \{8, 16, 128, 512, 768\}$ to find the optimal value. Additional details regarding the experimental setup can be found in Appendix A.

5. Experiments and Results

We begin by evaluating the choice of APLA’s core components, focusing first on identifying the most crucial layer for adaptation—the projection layer W_O —and how to select which parameters to tune within it. We then benchmark APLA against several other methods on standard classification, detection, and segmentation tasks, including low-data settings and out-of-distribution datasets. Additionally, we assess APLA across various model capacities, archi-

tectures, and foundation models. Finally, we evaluate its computational efficiency and explore how other adaptation techniques can benefit from our findings on the importance of the projection layer W_O .

5.1. Choosing APLA’s Components

Identifying which component to tune Previous work suggests that certain types of layers play a larger role in transfer learning [38, 47, 50, 55, 65]. To identify the optimal components for APLA, we systematically investigate the effect of tuning different ViT components individually, keeping all other layers frozen.

Table 1 and Figure 2 present results across four mainstream datasets representing diverse domains, tasks, and data availabilities. We find that tuning the projection layer W_O yields the best performance, even outperforming full-network fine-tuning. The clear advantage of W_O over other ViT components leads us to adopt it as the default layer to tune in APLA.

Identifying which parameters to tune Motivated by the effectiveness of low-rank adaptation methods, we explore strategies to economize APLA by selecting specific parameters in W_O for adaptation. We evaluate various strategies, including selecting columns with the largest gradients, activations, and weight magnitudes, as well as selecting the columns randomly.

We report our findings in Table 2. Surprisingly, tuning

Table 4. *Low-data settings*. We benchmark on VTAB-1k which contains 19 low-data tasks grouped across three domains.

	ViT-B				Swin-B			
	Natrl.	Spec.	Struc.	Average	Natrl.	Spec.	Struc.	Average
FINETUNE	75.9	83.4	47.6	69.0	79.1	86.2	59.7	75.0
LINEAR	68.9	77.2	26.9	57.7	73.5	80.8	33.5	62.6
MLP	67.8	72.8	30.6	57.1	73.6	75.2	35.7	61.5
PARTIAL	69.4	78.5	34.2	60.7	73.1	81.7	35.0	63.3
BITFIT	73.3	78.3	44.1	65.2	74.2	80.1	42.4	65.6
ADAPTER	79.0	84.1	58.5	73.9	81.7	87.3	61.2	76.7
ADAPTFORMER	80.6	85.4	58.8	74.9	—	—	—	—
VPT-SHALLOW	76.8	79.7	47.0	67.8	79.9	82.5	37.8	66.7
VPT-DEEP	78.5	82.4	55.0	72.0	76.8	84.5	53.4	71.6
E ² VPT	80.0	84.4	57.4	73.9	<u>83.3</u>	85.0	57.4	75.2
SSF	81.6	86.6	59.0	75.7	—	—	—	—
LoRA	79.5	84.6	60.5	74.8	81.7	87.2	60.1	76.3
SPT-ADAPTER	82.0	85.8	61.4	76.4	83.0	87.3	<u>62.1</u>	<u>77.5</u>
SPT-LoRA	81.9	85.9	61.3	76.4	83.1	<u>87.4</u>	60.4	77.2
NOAH	80.2	84.9	61.3	75.5	—	—	—	—
CONSOLIDATOR	82.4	86.3	60.9	76.5	—	—	—	—
FACT-TK	80.6	85.3	60.7	75.5	—	—	—	—
FACT-TT	80.6	85.0	60.5	75.3	83.1	86.9	62.1	77.4
ARC	81.8	87.0	61.4	76.7	79.0	86.6	59.9	75.2
RLRR	<u>83.7</u>	<u>87.3</u>	61.8	<u>77.6</u>	81.3	86.7	59.0	75.7
GPS	<u>83.7</u>	86.8	<u>61.9</u>	77.5	—	—	—	—
APLA	84.6	88.5	62.7	78.6	84.4	87.8	65.9	79.4

a random subset of columns in W_O performs on par with more sophisticated selection methods. This suggests that, within the projection layer W_O , the specific choice of tunable columns is less critical. For APLA we choose the random selection approach because it may better utilize feature redundancy across attention heads and achieves a slight advantage in performance without added computational cost.

5.2. Benchmarking APLA

Mainstream classification tasks We benchmark APLA against other methods across 21 diverse image classification tasks, including superordinate classification, fine-grained classification, scene recognition, satellite imagery, and medical image analysis. Table 3 presents the results. On average, APLA outperforms all other methods, showing a 0.6% improvement over the second-best method, ADAPTFORMER. It ranks as the top or second-best method on 18 out of 21 datasets, consistently demonstrating strong performance across different classification tasks.

APLA in low-data settings Foundation model adaptation is especially valuable in low-data scenarios, where reusing pretrained features is essential, as randomly initialized models tend to underperform [18, 37, 48]. We evaluate APLA in this regime using the VTAB-1k benchmark, which includes 19 datasets, each with only 1,000 samples. We use ViT-B and Swin-B pretrained on IMAGENET-21K and report average performance across three domains: natural, specialized, and structured. As shown in Table 4, APLA outperforms all other methods, achieving at least a 1% im-

Table 5. *OOD robustness*. We assess robustness to OOD data by adapting on ImageNet-1K and testing on ImageNet-A, ImageNet-R, and ImageNet-C.

	ImageNet-1K Acc. (↑)	ImageNet-A Acc. (↑)	ImageNet-R Acc. (↑)	ImageNet-C mCE (↓)
FINETUNE	83.6	34.5	51.3	46.5
LINEAR	82.0	33.9	52.9	46.9
ADAPTER	82.7	42.2	54.1	42.7
BITFIT	82.7	42.1	55.9	41.9
VPT-SHALLOW	82.1	30.9	53.7	46.9
VPT-DEEP	82.5	39.1	53.5	43.1
SSF	83.1	45.9	<u>56.8</u>	<u>41.5</u>
GPS	<u>83.9</u>	<u>46.1</u>	57.0	42.0
APLA	84.0	46.9	55.5	32.9

Table 6. *Segmentation and detection*. Results for ADE20K semantic segmentation (SETR-PUP [70] with a ViT-Large backbone) and COCO object detection & instance segmentation (Mask R-CNN [24] with a Swin-Tiny backbone).

	ADE20K		COCO					
	mIoU (SS)	mIoU (MS)	AP ^{bb}	AP ^{bb} ₅₀	AP ^{bb} ₇₅	AP ^m	AP ^m ₅₀	AP ^m ₇₅
BITFIT	43.4	45.3	33.7	57.8	35.0	32.7	54.7	33.9
VPT-DEEP	42.1	44.1	33.8	57.6	35.3	32.5	54.5	33.9
SSF	<u>45.6</u>	47.4	34.9	58.9	36.1	33.5	55.8	34.7
LoRA	43.9	45.9	37.1	60.9	39.5	35.2	57.7	37.2
ADAPTER	44.4	46.6	<u>37.6</u>	<u>61.1</u>	<u>40.2</u>	<u>35.6</u>	<u>58.2</u>	<u>37.8</u>
ADAPTFORMER	44.3	46.2	35.1	59.1	36.9	33.8	56.0	35.6
SPT-ADAPTER	45.2	47.2	—	—	—	—	—	—
SPT-LoRA	45.4	<u>47.5</u>	—	—	—	—	—	—
APLA	48.3	49.5	38.1	61.8	40.9	35.9	58.7	37.9

provement across these domains. Visualizations [59] of the [CLS] embeddings of different adaptation methods from these experiments are provided in Figure 9 in the Appendix.

Out-of-distribution robustness While APLA has shown strong performance across various settings, its robustness under domain shifts and adversarial examples remains to be assessed. Using a foundation model pretrained on ImageNet-21K, tuned on ImageNet-1K with various adaptation methods, we evaluate on ImageNet-A [27], ImageNet-R [26], and ImageNet-C [25]. As shown in Table 5, APLA outperforms other methods overall, achieving an 8.6% improvement in mean corruption error (mCE) on ImageNet-C. Notably, APLA and most other adaptation methods outperform full fine-tuning across all OOD datasets, highlighting the potential of efficient adaptation methods for OOD tasks.

Segmentation & Detection Tasks We evaluate APLA on semantic segmentation, object detection, and instance segmentation. For semantic segmentation, we use SETR-PUP [70] with a ViT-Large backbone pre-trained on IMAGENET-21K, reporting mean Intersection over Union (mIoU) for single-scale (SS) and multi-scale (MS) evaluations on ADE20K, as in [23, 31]. For object detection and instance segmentation, we use Mask R-CNN [24] with

Table 7. *Impact of pre-training strategy.* ViT-B pre-trained with IMAGENET-21K and OPENCLIP, then adapted to various tasks.

	IMAGENET-21K					OPENCLIP				
	Birds	Cars	AID	ISIC	Average	Birds	Cars	AID	ISIC	Average
FINETUNE	82.7	84.5	<u>91.7</u>	<u>84.0</u>	85.7	79.0	94.7	95.6	84.9	<u>88.6</u>
LINEAR	75.9	51.3	81.0	51.2	64.9	73.7	94.5	95.0	54.2	79.4
MLP	77.3	54.9	81.2	61.7	68.8	73.6	93.8	95.0	68.7	82.8
PARTIAL	77.8	66.2	81.1	46.6	67.9	73.8	94.4	95.2	54.9	79.6
BitFit	84.2	79.4	90.5	73.0	81.8	79.2	95.0	<u>95.8</u>	72.7	85.7
ADAPTER	84.3	68.6	90.0	80.6	80.9	79.2	95.0	95.2	<u>83.9</u>	88.3
ADAPTFORMER	78.8	83.1	90.1	81.2	83.3	80.0	95.0	95.5	82.4	88.2
VPT-SHALLOW	78.8	68.7	85.9	65.0	74.6	73.8	94.7	95.1	54.6	79.6
VPT-DEEP	84.2	83.6	89.0	74.8	82.9	73.6	94.5	95.1	54.6	79.5
E ² VPT	84.6	82.8	88.4	78.6	83.6	77.7	<u>95.1</u>	95.9	73.6	85.6
SSF	85.7	89.2	90.9	78.4	86.1	79.9	94.9	95.7	76.1	86.7
LoRA	<u>85.6</u>	83.2	91.0	83.5	85.8	79.0	94.1	95.0	83.2	87.8
SPT-ADAPTER	83.3	86.2	90.8	75.7	84.0	76.0	94.8	95.4	76.4	85.7
SPT-LoRA	83.4	87.3	90.0	76.2	84.2	75.9	94.9	95.1	77.4	85.8
FACT-TK	80.3	84.0	91.1	79.3	83.7	79.2	94.9	95.0	80.7	87.5
FACT-TT	79.2	82.4	90.9	77.7	82.6	78.5	94.9	95.4	77.2	86.5
ARC	85.7	89.5	90.8	79.2	<u>86.3</u>	79.5	<u>95.1</u>	95.1	79.0	87.2
RLRR	85.3	<u>90.4</u>	91.1	77.5	86.1	80.0	94.9	<u>95.8</u>	79.5	87.6
APLA	85.2	90.5	94.3	84.9	88.7	79.1	95.2	95.9	85.5	88.9

a Swin-Tiny backbone pre-trained on IMAGENET-1K, following [42, 44], and report mean Average Precision (AP) for bounding box (AP^{bb}) and mask (AP^m) predictions on MS COCO [43]. Additional details are in Appendix A. As shown in Table 6, APLA surpasses all other adaptation methods, with particularly strong results for semantic segmentation.

Different foundation model types and capacities. We evaluate APLA’s versatility across foundation model training strategies, capacities, and architectures, using both supervised IMAGENET-21K and semi-supervised OPENCLIP ViT-B models, as well as Swin transformers [44]. To assess scalability, we test ViT models of varying sizes (ViT-S, ViT-B, ViT-L, and ViT-g).

As shown in Tables 4, 7, and 8, APLA consistently outperforms other methods regardless of pretraining, model size, or architecture, maintaining strong performance where other methods show inconsistent performance.

Applying other adaptation methods on W_O In Section 5.1 we showed that W_O is the most impactful component to adapt—surpassing full fine-tuning—and in Section 5.2 we show that, when targeted in APLA, it outperforms other adaptation methods. We now explore what happens if other adaptation methods are applied to W_O . Do they improve performance when targeted to this layer? Does the low-rank adaptation strategy we propose for APLA prevail against other adaptation methods that target the same layer? Using ViT-B pretrained with DINOv2, we apply LoRA [29], FACT [32], and ADAPTFORMER [6] on W_O and compare on Birds, Cars, AID, ISIC, and VTAB-1k.

Table 8. *Impact of model capacity.* Results are averaged across NABirds, StanfordCars, AID, and ISIC2019 using DINOv2 pre-trained models. Detailed results can be found in Appendix B.1.

	ViT-S	ViT-B	ViT-L	ViT-g
FINETUNE	86.2	90.7	<u>92.1</u>	92.6
LINEAR	76.1	80.4	83.6	85.5
MLP	80.9	84.6	86.2	87.8
PARTIAL	75.8	80.4	83.6	85.2
BitFit	84.8	88.7	90.0	91.8
ADAPTER	87.9	90.3	91.9	92.3
ADAPTFORMER	87.2	90.6	91.7	<u>92.8</u>
VPT-SHALLOW	82.8	86.4	88.3	88.9
VPT-DEEP	84.0	88.2	90.2	91.9
E ² VPT	84.2	88.1	90.9	91.7
SSF	84.7	89.2	91.0	91.9
LoRA	87.1	<u>90.8</u>	<u>92.1</u>	92.6
SPT-ADAPTER	87.2	89.7	90.0	89.5
SPT-LoRA	87.6	89.6	90.5	89.4
FACT-TK	86.9	90.3	91.5	92.0
FACT-TT	85.4	89.1	91.3	91.6
ARC	86.0	89.7	91.1	91.9
RLRR	84.4	89.3	91.8	92.3
APLA	88.0	91.6	92.9	93.4

As shown in Table 9, applying other adaptation methods to W_O generally improves performance, solidifying the importance of the W_O layer. *Critically, APLA still outperforms other leading approaches when they are applied to W_O , suggesting there is an advantage to our simple low-rank adaptation strategy using random partial gradients.*

Computational cost We analyze the computational costs of adaptation methods by measuring GPU memory footprint, parameter count, and throughput during training and inference. Results for training are shown in Figure 3, with additional results and details in the Appendix B. APLA demonstrates significant efficiency improvements, reducing memory usage and boosting training throughput, with no extra inference cost. Figure 1 further illustrates that APLA’s memory savings increase with model size, even surpassing BitFit, which tunes only bias parameters. Figure 5 in the Appendix reports parameter count, showing that APLA appears more costly than many methods according to this metric. However, as noted by prior work [4, 13], parameter count is misleading in assessing computational efficiency. In practice, APLA *remains the most efficient method*, consistently outperforming others in GPU memory usage and throughput during both training and inference.

We also examine how increasing the rank r affects computational requirements for APLA and other low-rank methods in Appendix B.3. In tasks with significant domain shifts, a higher r may be needed to re-weight features and bridge the gap between pretraining and the target domain. By leveraging existing model parameters, APLA keeps memory and throughput costs nearly fixed, even at higher ranks, unlike other approaches that become increasingly expensive as r increases.

Table 9. *Applying other adaptation methods on W_O .* Competing methods are applied to W_O , isolating the effect of APLA’s low-rank adaptation strategy. “Natural”, “Specialized”, and “Structured” indicate average performance across respective VTAB groups. Notably, LORA and ADAPTFORMER would be improved if they were placed at W_O rather than their default locations.

Method	Adaptation	Birds	Cars	AID	ISIC	Natrl.	Spec.	Struc.	Average
LORA	Default	87.5	93.4	<u>95.4</u>	86.5	83.4	86.5	63.1	78.2
	On W_O	87.7	93.5	<u>95.1</u>	<u>87.9</u>	83.7	<u>87.6</u>	62.6	78.3
ADAPTF.	Default	88.4	93.1	<u>95.4</u>	<u>85.6</u>	84.0	87.2	59.8	77.3
	On W_O	88.4	93.6	<u>95.3</u>	87.1	84.2	87.2	61.6	78.1
FACT	Default	87.8	93.0	<u>95.4</u>	85.1	<u>84.7</u>	87.4	64.5	<u>79.1</u>
	On W_O	<u>88.0</u>	<u>93.8</u>	95.3	86.5	84.4	87.2	<u>63.8</u>	78.8
APLA	On W_O	<u>88.0</u>	94.0	96.0	88.2	85.0	88.2	63.9	79.4

6. Discussion

APLA establishes a new state-of-the-art for efficient model adaptation across a wide range of classification, segmentation, and detection tasks, showing resilience in low-data and out-of-distribution scenarios. It achieved top performance across model types, capacities, and pretraining methods – a level of versatility that no other adaptation method maintained across such varied conditions. Moreover, APLA excels in computational efficiency, significantly reducing memory and processing requirements.

APLA offers several practical advantages in addition to its exceptional performance. It is simple to implement, requiring no architectural changes or added parameters which may be sensitive to initialization. It eliminates the need to search for which parameters to update. APLA’s simplicity makes it easy to work with. APLA also supports flexible layer adaptation, allowing partial or full layer updates depending on the need, all with minimal computational overhead. Finally, as demonstrated in Section 5.2, APLA’s core insights can be used to enhance other adaptation methods, *e.g.*, applying ADAPTFORMER solely on W_O gives a 1% boost in performance.

What makes APLA so effective? Although we don’t have a definitive answer, we offer two possible explanations. One is the targeting of W_O . Foundation models encode a rich set of features robust to various tasks. However, each task benefits from a unique composition of these features, making feature re-weighting essential. This is precisely the role of W_O , which re-weights the contribution of features across all attention heads. Figure 2 reveals that other top-performing ViT components serve similar functions: W_V re-weights the attention output within each head, while W_O operates across all heads. Given this, one might expect W_{FC_1} and W_{FC_2} in the MLP block to play a more critical role, but they are positioned further downstream, with W_O and normalization layers modifying the features before they reach the MLP block.

A second explanation for APLA’s effectiveness lies in

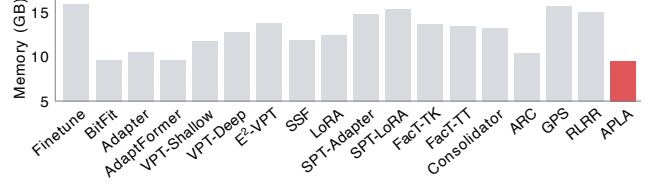


Figure 3. *Computational cost.* We report the memory footprint of various adaptation methods during training with a batch size of 64. Results for parameter count, memory, and throughput during training and inference are provided in Appendix B.2.

the simplicity of its low-rank adaptation using randomly selected gradient updates. Other approaches to use heuristics to select parameters, *e.g.* based on large weights, activations, or gradients may be suboptimal for foundation models, which are highly over-parameterized and exhibit feature redundancy. Selection based on large gradients or weights may not capture the most relevant features, could bias adaptation toward redundant or overly specific features, and lead to overfitting. By re-weighting a broader range of features, random selection makes APLA equally or even more effective in contexts of high feature redundancy, as shown in Table 2.

Why does APLA often outperform full fine-tuning? We speculate that, in low-data settings, full fine-tuning may distort pre-trained features to fit the limited training set, leading to overfitting—an issue less pronounced with partial tuning of W_O .

Limitations & future work While our experiments are extensive, certain aspects remain unexplored. Our study focuses on identifying the single most important ViT component for adaptation rather than multiple components. An exhaustive search would be computationally prohibitive, and a constrained search, resembling a NAS, may yield undesirable task-specific combinations [68]. We also did not examine how the choice of r might vary with data availability or information density; richer data may support a larger r and enhance adaptability. Lastly, APLA’s susceptibility to catastrophic forgetting remains untested—unlike adapter-based methods, which can be stored separately, APLA directly modifies the foundation model, potentially impacting retention of prior knowledge.

7. Conclusion

We introduced APLA, a simple yet effective method for adapting ViTs by tuning only a randomly selected subset of projection layer columns. Extensive experiments show that APLA achieves state-of-the-art performance while reducing computational costs, making it highly practical. Our results highlight that in over-parameterized models, efficiency doesn’t require added complexity – a simple targeted re-weighting of existing features can be even more powerful.

References

- [1] Jimmy Lei Ba. Layer normalization. *arXiv preprint arXiv:1607.06450*, 2016. 3
- [2] Thomas Berg, Jiongxin Liu, Seung Woo Lee, Michelle L Alexander, David W Jacobs, and Peter N Belhumeur. Birdsnap: Large-scale fine-grained visual categorization of birds. In *Proceedings of the IEEE conference on computer vision and pattern recognition*, pages 2011–2018, 2014. 4
- [3] Rishi Bommasani, Drew A Hudson, Ehsan Adeli, Russ Altman, Simran Arora, Sydney von Arx, Michael S Bernstein, Jeannette Bohg, Antoine Bosselut, Emma Brunskill, et al. On the opportunities and risks of foundation models. *arXiv preprint arXiv:2108.07258*, 2021. 2
- [4] Han Cai, Chuang Gan, Ligeng Zhu, and Song Han. Tinytl: Reduce memory, not parameters for efficient on-device learning. *Advances in Neural Information Processing Systems*, 33:11285–11297, 2020. 7, A2
- [5] Kai Chen, Jiaqi Wang, Jiangmiao Pang, Yuhang Cao, Yu Xiong, Xiaoxiao Li, Shuyang Sun, Wansen Feng, Ziwei Liu, Jiarui Xu, Zheng Zhang, Dazhi Cheng, Chenchen Zhu, Tianheng Cheng, Qijie Zhao, Buyu Li, Xin Lu, Rui Zhu, Yue Wu, Jifeng Dai, Jingdong Wang, Jianping Shi, Wanli Ouyang, Chen Change Loy, and Dahua Lin. MMDetection: Open mmlab detection toolbox and benchmark. *arXiv preprint arXiv:1906.07155*, 2019. A1
- [6] Shoufa Chen, Chongjian Ge, Zhan Tong, Jiangliu Wang, Yibing Song, Jue Wang, and Ping Luo. Adaptformer: Adapting vision transformers for scalable visual recognition. *Advances in Neural Information Processing Systems*, 35:16664–16678, 2022. 1, 2, 4, 5, 7, A1, A2
- [7] Gong Cheng, Junwei Han, and Xiaoqiang Lu. Remote sensing image scene classification: Benchmark and state of the art. *Proceedings of the IEEE*, 105(10):1865–1883, 2017. 4
- [8] Mircea Cimpoi, Subhransu Maji, Iasonas Kokkinos, Sammy Mohamed, and Andrea Vedaldi. Describing textures in the wild. In *Proceedings of the IEEE conference on computer vision and pattern recognition*, pages 3606–3613, 2014. 4
- [9] Noel CF Codella, David Gutman, M Emre Celebi, Brian Helba, Michael A Marchetti, Stephen W Dusza, Aadi Kalloo, Konstantinos Liopyris, Nabin Mishra, Harald Kittler, et al. Skin lesion analysis toward melanoma detection: A challenge at the 2017 international symposium on biomedical imaging (isbi), hosted by the international skin imaging collaboration (isic). In *2018 IEEE 15th international symposium on biomedical imaging (ISBI 2018)*, pages 168–172. IEEE, 2018. 4
- [10] Marc Combalia, Noel CF Codella, Veronica Rotemberg, Brian Helba, Veronica Vilaplana, Ofer Reiter, Cristina Carrera, Alicia Barreiro, Allan C Halpern, Susana Puig, et al. Bcn20000: Dermoscopic lesions in the wild. *arXiv preprint arXiv:1908.02288*, 2019. 4
- [11] MMsegmentation Contributors. MMsegmentation: Openmmlab semantic segmentation toolbox and benchmark. <https://github.com/open-mmlab/mmdetection>, 2020. A1
- [12] Yin Cui, Yang Song, Chen Sun, Andrew Howard, and Serge Belongie. Large scale fine-grained categorization and domain-specific transfer learning. In *Proceedings of the IEEE conference on computer vision and pattern recognition*, pages 4109–4118, 2018. 2
- [13] Mostafa Dehghani, Anurag Arnab, Lucas Beyer, Ashish Vaswani, and Yi Tay. The efficiency misnomer. *arXiv preprint arXiv:2110.12894*, 2021. 7, A2
- [14] Mostafa Dehghani, Josip Djolonga, Basil Mustafa, Piotr Padlewski, Jonathan Heek, Justin Gilmer, Andreas Peter Steiner, Mathilde Caron, Robert Geirhos, Ibrahim Alabdulmohsin, et al. Scaling vision transformers to 22 billion parameters. In *International Conference on Machine Learning*, pages 7480–7512. PMLR, 2023. 2
- [15] Jia Deng, Wei Dong, Richard Socher, Li-Jia Li, Kai Li, and Li Fei-Fei. Imagenet: A large-scale hierarchical image database. In *2009 IEEE conference on computer vision and pattern recognition*, pages 248–255. Ieee, 2009. 4, A1
- [16] Wei Dong, Dawei Yan, Zhijun Lin, and Peng Wang. Efficient adaptation of large vision transformer via adapter recomposing. *Advances in Neural Information Processing Systems*, 36, 2024. 2, 4, 5, A1
- [17] Wei Dong, Xing Zhang, Bihui Chen, Dawei Yan, Zhijun Lin, Qingsen Yan, Peng Wang, and Yang Yang. Low-rank rescaled vision transformer fine-tuning: A residual design approach. In *Proceedings of the IEEE/CVF Conference on Computer Vision and Pattern Recognition*, pages 16101–16110, 2024. 2, 4, 5, A1
- [18] Alexey Dosovitskiy. An image is worth 16x16 words: Transformers for image recognition at scale. *arXiv preprint arXiv:2010.11929*, 2020. 4, 5, 6, A1
- [19] Li Fei-Fei, Robert Fergus, and Pietro Perona. One-shot learning of object categories. *IEEE transactions on pattern analysis and machine intelligence*, 28(4):594–611, 2006. 4
- [20] Gregory Griffin, Alex Holub, and Pietro Perona. Caltech-256 object category dataset, 2007. 4
- [21] Cheng Han, Qifan Wang, Yiming Cui, Zhiwen Cao, Wenguan Wang, Siyuan Qi, and Dongfang Liu. E² 2vpt: An effective and efficient approach for visual prompt tuning. *arXiv preprint arXiv:2307.13770*, 2023. 2, 4, 5, A1
- [22] Tianxiang Hao, Hui Chen, Yuchen Guo, and Guiguang Ding. Consolidator: Mergeable adapter with grouped connections for visual adaptation. *arXiv preprint arXiv:2305.00603*, 2023. 2, 4
- [23] Haoyu He, Jianfei Cai, Jing Zhang, Dacheng Tao, and Bohan Zhuang. Sensitivity-aware visual parameter-efficient fine-tuning. In *Proceedings of the IEEE/CVF International Conference on Computer Vision*, pages 11825–11835, 2023. 1, 2, 4, 6, A1
- [24] Kaiming He, Georgia Gkioxari, Piotr Dollár, and Ross Girshick. Mask r-cnn. In *Proceedings of the IEEE international conference on computer vision*, pages 2961–2969, 2017. 6, A1
- [25] Dan Hendrycks and Thomas Dietterich. Benchmarking neural network robustness to common corruptions and perturbations. *arXiv preprint arXiv:1903.12261*, 2019. 4, 6
- [26] Dan Hendrycks, Steven Basart, Norman Mu, Saurav Kadavath, Frank Wang, Evan Dorundo, Rahul Desai, Tyler Zhu, Samyak Parajuli, Mike Guo, et al. The many faces of robustness: A critical analysis of out-of-distribution generalization.

- In *Proceedings of the IEEE/CVF international conference on computer vision*, pages 8340–8349, 2021. 4, 6
- [27] Dan Hendrycks, Kevin Zhao, Steven Basart, Jacob Steinhardt, and Dawn Song. Natural adversarial examples. In *Proceedings of the IEEE/CVF conference on computer vision and pattern recognition*, pages 15262–15271, 2021. 4, 6
- [28] Neil Houlsby, Andrei Giurgiu, Stanislaw Jastrzebski, Bruna Morrone, Quentin De Laroussilhe, Andrea Gesmundo, Mona Attariyan, and Sylvain Gelly. Parameter-efficient transfer learning for nlp. In *International conference on machine learning*, pages 2790–2799. PMLR, 2019. 2, 4
- [29] Edward J Hu, Yelong Shen, Phillip Wallis, Zeyuan Allen-Zhu, Yuanzhi Li, Shean Wang, Lu Wang, and Weizhu Chen. Lora: Low-rank adaptation of large language models. *arXiv preprint arXiv:2106.09685*, 2021. 1, 2, 3, 4, 5, 7, A1
- [30] Gabriel Ilharco, Mitchell Wortsman, Ross Wightman, Cade Gordon, Nicholas Carlini, Rohan Taori, Achal Dave, Vaishaal Shankar, Hongseok Namkoong, John Miller, Hananeh Hajishirzi, Ali Farhadi, and Ludwig Schmidt. Openclip, 2021. If you use this software, please cite it as below. 2, 4
- [31] Menglin Jia, Luming Tang, Bor-Chun Chen, Claire Cardie, Serge Belongie, Bharath Hariharan, and Ser-Nam Lim. Visual prompt tuning. In *European Conference on Computer Vision*, pages 709–727. Springer, 2022. 1, 2, 4, 5, 6, A1, A2
- [32] Shibo Jie and Zhi-Hong Deng. Fact: Factor-tuning for lightweight adaptation on vision transformer. In *Proceedings of the AAAI conference on artificial intelligence*, pages 1060–1068, 2023. 1, 2, 3, 4, 5, 7, A1
- [33] Sohier Dane Karthik, Maggie. Aptos 2019 blindness detection, 2019. 4
- [34] Jakob Nikolas Kather, Cleo-Aron Weis, Francesco Bianconi, Susanne M Melchers, Lothar R Schad, Timo Gaiser, Alexander Marx, and Frank Gerrit Zöllner. Multi-class texture analysis in colorectal cancer histology. *Scientific reports*, 6(1): 1–11, 2016. 4
- [35] Daniel S Kermany, Michael Goldbaum, Wenjia Cai, Carolina CS Valentim, Huiying Liang, Sally L Baxter, Alex McKeown, Ge Yang, Xiaokang Wu, Fangbing Yan, et al. Identifying medical diagnoses and treatable diseases by image-based deep learning. *cell*, 172(5):1122–1131, 2018. 4
- [36] Aditya Khosla, Nityananda Jayadevaprakash, Bangpeng Yao, and Fei-Fei Li. Novel dataset for fine-grained image categorization: Stanford dogs. In *Proc. CVPR workshop on fine-grained visual categorization (FGVC)*. Citeseer, 2011. 4
- [37] Alexander Kolesnikov, Lucas Beyer, Xiaohua Zhai, Joan Puigcerver, Jessica Yung, Sylvain Gelly, and Neil Houlsby. Big transfer (bit): General visual representation learning. In *Computer Vision–ECCV 2020: 16th European Conference, Glasgow, UK, August 23–28, 2020, Proceedings, Part V 16*, pages 491–507. Springer, 2020. 6
- [38] Emir Konuk, Christos Matsoukas, Moein Sorkhei, Phitchapha Lertsiravarameth, and Kevin Smith. Learning from offline foundation features with tensor augmentations. In *The Thirty-eighth Annual Conference on Neural Information Processing Systems*, 2024. 5
- [39] Jonathan Krause, Michael Stark, Jia Deng, and Li Fei-Fei. 3d object representations for fine-grained categorization. In *Proceedings of the IEEE international conference on computer vision workshops*, pages 554–561, 2013. 4
- [40] Alex Krizhevsky, Geoffrey Hinton, et al. Learning multiple layers of features from tiny images, 2009. 4
- [41] Rebecca Sawyer Lee, Francisco Gimenez, Assaf Hoogi, Kanae Kawai Miyake, Mia Gorovoy, and Daniel L Rubin. A curated mammography data set for use in computer-aided detection and diagnosis research. *Scientific data*, 4(1):1–9, 2017. 4
- [42] Dongze Lian, Daquan Zhou, Jiashi Feng, and Xinchao Wang. Scaling & shifting your features: A new baseline for efficient model tuning. *Advances in Neural Information Processing Systems*, 35:109–123, 2022. 1, 2, 4, 7, A1, A2
- [43] Tsung-Yi Lin, Michael Maire, Serge Belongie, James Hays, Pietro Perona, Deva Ramanan, Piotr Dollár, and C Lawrence Zitnick. Microsoft coco: Common objects in context. In *Computer Vision–ECCV 2014: 13th European Conference, Zurich, Switzerland, September 6–12, 2014, Proceedings, Part V 13*, pages 740–755. Springer, 2014. 4, 7, A1
- [44] Ze Liu, Yutong Lin, Yue Cao, Han Hu, Yixuan Wei, Zheng Zhang, Stephen Lin, and Baining Guo. Swin transformer: Hierarchical vision transformer using shifted windows. In *Proceedings of the IEEE/CVF international conference on computer vision*, pages 10012–10022, 2021. 2, 4, 7, A1
- [45] Ilya Loshchilov and Frank Hutter. Decoupled weight decay regularization. *arXiv preprint arXiv:1711.05101*, 2017. 5, A1
- [46] Subhansu Maji, Esa Rahtu, Juho Kannala, Matthew Blaschko, and Andrea Vedaldi. Fine-grained visual classification of aircraft. *arXiv preprint arXiv:1306.5151*, 2013. 4
- [47] Christos Matsoukas, Johan Fredin Haslum, Moein Sorkhei, Magnus Söderberg, and Kevin Smith. What makes transfer learning work for medical images: Feature reuse & other factors. In *Proceedings of the IEEE/CVF Conference on Computer Vision and Pattern Recognition*, pages 9225–9234, 2022. 5
- [48] Christos Matsoukas, Johan Fredin Haslum, Magnus Söderberg, and Kevin Smith. Pretrained vits yield versatile representations for medical images. *arXiv preprint arXiv:2303.07034*, 2023. 6
- [49] Basil Mustafa, Aaron Loh, Jan Freyberg, Patricia MacWilliams, Megan Wilson, Scott Mayer McKinney, Marcin Sieniek, Jim Winkens, Yuan Liu, Peggy Bui, et al. Supervised transfer learning at scale for medical imaging. *arXiv preprint arXiv:2101.05913*, 2021. 2
- [50] Behnam Neyshabur, Hanie Sedghi, and Chiyuan Zhang. What is being transferred in transfer learning? *Advances in neural information processing systems*, 33:512–523, 2020. 5
- [51] Maxime Oquab, Timothée Darcet, Théo Moutakanni, Huy Vo, Marc Szafraniec, Vasil Khalidov, Pierre Fernandez, Daniel Haziza, Francisco Massa, Alaaeldin El-Nouby, et al. Dinov2: Learning robust visual features without supervision. *arXiv preprint arXiv:2304.07193*, 2023. 2, 5, A1
- [52] Omkar M Parkhi, Andrea Vedaldi, Andrew Zisserman, and CV Jawahar. Cats and dogs. In *2012 IEEE conference on*

- computer vision and pattern recognition*, pages 3498–3505. IEEE, 2012. 4
- [53] Adam Paszke, Sam Gross, Francisco Massa, Adam Lerer, James Bradbury, Gregory Chanan, Trevor Killeen, Zeming Lin, Natalia Gimelshein, Luca Antiga, et al. Pytorch: An imperative style, high-performance deep learning library. *Advances in neural information processing systems*, 32, 2019. A1
- [54] Ariadna Quattoni and Antonio Torralba. Recognizing indoor scenes. In *2009 IEEE conference on computer vision and pattern recognition*, pages 413–420. IEEE, 2009. 4
- [55] Ali Sharif Razavian, Hossein Azizpour, Josephine Sullivan, and Stefan Carlsson. Cnn features off-the-shelf: an astounding baseline for recognition. In *Proceedings of the IEEE conference on computer vision and pattern recognition workshops*, pages 806–813, 2014. 5
- [56] Jan-Martin O Steitz and Stefan Roth. Adapters strike back. In *Proceedings of the IEEE/CVF Conference on Computer Vision and Pattern Recognition*, pages 23449–23459, 2024. 2
- [57] Hugo Touvron, Matthieu Cord, Alexandre Sablayrolles, Gabriel Synnaeve, and Hervé Jégou. Going deeper with image transformers. In *Proceedings of the IEEE/CVF international conference on computer vision*, pages 32–42, 2021. 3
- [58] Philipp Tschandl, Cliff Rosendahl, and Harald Kittler. The ham10000 dataset, a large collection of multi-source dermatoscopic images of common pigmented skin lesions. *Scientific data*, 5(1):1–9, 2018. 4
- [59] Laurens Van der Maaten and Geoffrey Hinton. Visualizing data using t-sne. *Journal of machine learning research*, 9 (11), 2008. 6, A2
- [60] Grant Van Horn, Steve Branson, Ryan Farrell, Scott Haber, Jessie Barry, Panos Ipeirotis, Pietro Perona, and Serge Belongie. Building a bird recognition app and large scale dataset with citizen scientists: The fine print in fine-grained dataset collection. In *Proceedings of the IEEE Conference on Computer Vision and Pattern Recognition*, pages 595–604, 2015. 4
- [61] A Vaswani. Attention is all you need. *Advances in Neural Information Processing Systems*, 2017. 2
- [62] Catherine Wah, Steve Branson, Peter Welinder, Pietro Perona, and Serge Belongie. The caltech-ucsd birds-200-2011 dataset. Technical Report CNS-TR-2011-001, California Institute of Technology, 2011. 4
- [63] Gui-Song Xia, Jingwen Hu, Fan Hu, Baoguang Shi, Xiang Bai, Yanfei Zhong, Liangpei Zhang, and Xiaoqiang Lu. Aid: A benchmark data set for performance evaluation of aerial scene classification. *IEEE Transactions on Geoscience and Remote Sensing*, 55(7):3965–3981, 2017. 4
- [64] Jianxiong Xiao, James Hays, Krista A Ehinger, Aude Oliva, and Antonio Torralba. Sun database: Large-scale scene recognition from abbey to zoo. In *2010 IEEE computer society conference on computer vision and pattern recognition*, pages 3485–3492. IEEE, 2010. 4
- [65] Jason Yosinski, Jeff Clune, Yoshua Bengio, and Hod Lipson. How transferable are features in deep neural networks? *Advances in neural information processing systems*, 27, 2014. 5
- [66] Elad Ben Zaken, Shauli Ravfogel, and Yoav Goldberg. Bitfit: Simple parameter-efficient fine-tuning for transformer-based masked language-models. *arXiv preprint arXiv:2106.10199*, 2021. 1, 2, 4
- [67] Xiaohua Zhai, Joan Puigcerver, Alexander Kolesnikov, Pierre Ruyssen, Carlos Riquelme, Mario Lucic, Josip Djolonga, Andre Susano Pinto, Maxim Neumann, Alexey Dosovitskiy, et al. A large-scale study of representation learning with the visual task adaptation benchmark. *arXiv preprint arXiv:1910.04867*, 2019. 4, 5
- [68] Yuanhan Zhang, Kaiyang Zhou, and Ziwei Liu. Neural prompt search. *arXiv preprint arXiv:2206.04673*, 2022. 1, 2, 4, 8
- [69] Zhi Zhang, Qizhe Zhang, Zijun Gao, Renrui Zhang, Ekaterina Shutova, Shiji Zhou, and Shanghang Zhang. Gradient-based parameter selection for efficient fine-tuning. In *Proceedings of the IEEE/CVF Conference on Computer Vision and Pattern Recognition*, pages 28566–28577, 2024. 1, 2, 4
- [70] Sixiao Zheng, Jiachen Lu, Hengshuang Zhao, Xiatian Zhu, Zekun Luo, Yabiao Wang, Yanwei Fu, Jianfeng Feng, Tao Xiang, Philip HS Torr, et al. Rethinking semantic segmentation from a sequence-to-sequence perspective with transformers. In *Proceedings of the IEEE/CVF conference on computer vision and pattern recognition*, pages 6881–6890, 2021. 2, 6, A1
- [71] Bolei Zhou, Hang Zhao, Xavier Puig, Sanja Fidler, Adela Barriuso, and Antonio Torralba. Scene parsing through ade20k dataset. In *Proceedings of the IEEE conference on computer vision and pattern recognition*, pages 633–641, 2017. 4, A1
- [72] Bolei Zhou, Hang Zhao, Xavier Puig, Tete Xiao, Sanja Fidler, Adela Barriuso, and Antonio Torralba. Semantic understanding of scenes through the ade20k dataset. *International Journal of Computer Vision*, 127(3):302–321, 2019. 4, A1

APLA: A Simple Adaptation Method for Vision Transformers

Supplementary Material

We provide additional experimental details and results.

- [A](#) includes additional experimental details.
 - In [Section A.1](#) we provide implementation details for classification tasks.
 - In [A.2](#) we provide experimental details for semantic segmentation tasks.
 - In [A.3](#) we provide experimental details for object detection and instance segmentation tasks.
- [Section B](#) includes additional experimental results.
 - In [B.1](#) we report additional results as the model’s capacity increases, including both classification performance and computational cost.
 - In [B.2](#) we report additional results on the computational costs of APLA and other adaptation methods during training and inference.
 - In [B.3](#) We examine the effect of rank r on computational requirements for different low-rank methods when applied solely to W_O during training.
 - In [B.4](#) we investigate the impact of applying APLA to an increasing number of ViT blocks.
 - In [B.5](#) we discuss the best r values for APLA.
 - In [B.6](#) we visualize and discuss the quality of output features produced by different adaptation methods.

A. Additional Experimental Details

A.1. Image Classification

To ensure fair comparison against other adaptation methods, we closely follow the implementations in [6, 16, 17, 21, 29, 31, 32]. For each dataset in the general classification tasks, either the official train/val/test splits were used, or we used the splits from [31]. For VTAB, the train/val/test splits are provided. All models were developed in PyTorch [53] and trained on Nvidia A100 GPUs using AdamW [45] optimizer. Unless stated otherwise, models were trained for 100 epochs using a cosine decay learning rate schedule with a 10-epoch warm-up, following previous works [16, 17, 21, 31, 32]. We perform grid-search to determine the hyper-parameters using the validation set of each dataset. We also perform a grid search to determine the appropriate r value in APLA for each dataset. For ViT-S, we search over $r \in \{8, 16, 128, 256, 384\}$. For ViT-B, we search over $r \in \{8, 16, 128, 512, 768\}$. For ViT-L, we search over $r \in \{8, 16, 128, 512, 1024\}$. For ViT-g, we search over $r \in \{8, 16, 128, 1024, 1536\}$.

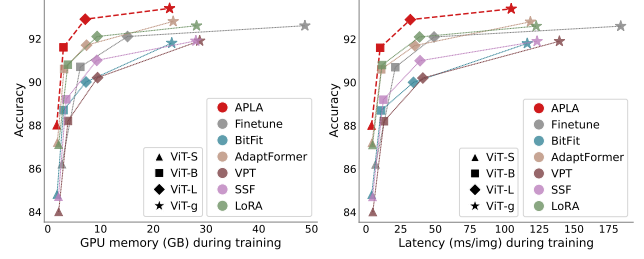


Figure 4. *Performance vs. compute cost.* We compare each method’s performance against GPU memory (left) and latency (right) during training across different model capacities.

A.2. Semantic Segmentation

For semantic segmentation we follow [23, 31] and conduct experiments on the ADE20K dataset [71, 72] using the SETR-PUP framework [70] with a ViT-Large [18] model pre-trained on IMAGENET-21K [15]. We report mean Intersection over Union (mIoU) scores for both single-scale (SS) and multi-scale (MS), following [23, 31]. Our implementation uses the *mmsegmentation* [11] library. We merely apply APLA on the default models of the library. All training configurations are kept unchanged.

A.3. Object Detection & Instance Segmentation

For object detection and instance segmentation tasks we follow [42, 44] and conduct experiments on the MS COCO dataset [43] using the Mask R-CNN framework [24] with a Swin-Tiny [44] model pre-trained on IMAGENET-1K [15]. We report mean Average Precision (AP) for both bounding boxes (AP^{bb}) and masks (AP^m) across multiple IoU thresholds and individual thresholds, following [42–44]. Our implementation uses the *mmdetection* [5] library. We merely apply APLA on the default models of the library. All training configurations are kept unchanged.

B. Additional Experimental Results

B.1. Detailed Results of Different Model Scales

To examine if APLA scales well with model size, we utilize ViT models of varying sizes (ViT-S, ViT-B, ViT-L, and ViT-g), pre-trained with DINOv2 [51]. Table 8 in the main text shows the average results of different adaptation methods across model scales, while Table 10 provides detailed per-dataset results. APLA appears to benefit from increased model capacity, performing exceptionally well with larger models. We further present a performance-efficiency trade-

Table 10. *Classification performance across different model sizes.* The **best** and second best results are highlighted.

	ViT-S					ViT-B					ViT-L					ViT-g				
	Birds	Cars	AID	ISIC	Average	Birds	Cars	AID	ISIC	Average	Birds	Cars	AID	ISIC	Average	Birds	Cars	AID	ISIC	Average
FINETUNE	77.5	91.9	91.7	<u>83.8</u>	86.2	85.2	94.4	95.4	<u>87.7</u>	90.7	88.2	<u>94.9</u>	95.9	89.2	<u>92.1</u>	90.0	<u>95.2</u>	96.5	88.8	92.6
LINEAR	81.3	83.1	88.5	51.5	76.1	86.6	88.4	91.2	55.3	80.4	89.1	89.8	93.4	62.1	83.6	90.2	91.0	93.6	67.3	85.5
MLP	80.6	83.1	88.8	71.1	80.9	86.4	88.3	91.6	71.9	84.6	88.9	89.9	92.9	73.0	86.2	89.9	91.0	93.1	77.1	87.8
PARTIAL	81.1	83.1	88.3	50.6	75.8	86.5	88.1	90.9	56.1	80.4	89.1	89.8	93.3	62.0	83.6	90.3	91.0	93.6	65.7	85.2
BitFit	83.1	89.7	93.1	73.2	84.8	87.9	92.5	95.2	79.0	88.7	90.4	93.8	95.8	80.1	90.0	90.8	94.5	95.9	85.8	91.8
ADAPTER	<u>83.2</u>	91.3	<u>93.3</u>	<u>83.8</u>	<u>87.9</u>	88.4	93.5	95.0	84.3	90.3	90.4	94.8	95.8	86.4	91.9	91.1	95.1	96.3	86.8	92.3
ADAPTFORMER	83.6	90.6	92.8	81.9	<u>87.2</u>	88.4	93.1	95.4	85.6	90.6	90.8	94.2	95.8	86.0	91.7	91.5	94.9	96.0	<u>88.9</u>	<u>92.8</u>
VPT-SHALLOW	81.7	86.3	91.3	72.0	82.8	86.7	90.6	91.6	76.5	86.4	89.0	91.6	93.0	79.7	88.3	89.8	92.1	95.1	78.7	88.9
VPT-DEEP	80.1	86.8	92.5	76.7	84.0	87.3	91.5	94.4	79.6	88.2	89.1	93.4	95.7	82.6	90.2	91.1	94.5	96.2	85.9	91.9
E ² VPT	80.0	87.6	91.9	77.3	84.2	86.6	91.2	93.7	80.9	88.1	89.5	93.8	95.8	84.3	90.9	91.2	94.5	95.9	85.3	91.7
SSF	81.7	89.5	92.7	74.9	84.7	88.1	92.7	95.3	80.7	89.2	<u>90.6</u>	94.0	95.9	83.5	91.0	91.0	94.5	95.9	86.3	91.9
LoRA	80.8	91.0	<u>93.3</u>	83.2	87.1	87.9	93.4	95.4	86.5	<u>90.8</u>	89.9	94.8	95.9	87.9	<u>92.1</u>	89.8	94.8	<u>96.7</u>	<u>88.9</u>	92.6
SPT-ADAPTER	83.0	91.0	<u>93.3</u>	81.4	87.2	88.1	93.1	<u>95.6</u>	82.1	<u>89.7</u>	<u>90.6</u>	93.4	95.6	<u>80.5</u>	90.0	90.7	93.2	95.0	79.0	89.5
SPT-LoRA	82.8	91.1	93.2	83.2	87.6	87.9	92.8	95.4	82.2	89.6	89.6	93.8	95.5	82.9	90.5	90.3	93.5	95.2	78.5	89.4
FACT-TK	82.5	90.6	92.9	81.7	86.9	87.8	93.0	95.4	85.1	90.3	<u>90.6</u>	94.5	<u>96.3</u>	84.4	91.5	91.6	95.1	96.1	85.3	92.0
FACT-TT	82.3	89.7	91.6	78.0	85.4	87.6	92.9	94.5	81.5	89.1	90.5	94.6	<u>96.3</u>	83.7	91.3	91.4	94.7	96.0	84.1	91.6
ARC	82.9	89.4	93.2	78.5	86.0	88.2	92.6	95.6	82.5	89.7	<u>90.6</u>	94.3	95.5	83.9	91.1	91.5	94.7	95.7	85.5	91.9
RLRR	82.4	89.5	<u>93.3</u>	72.2	84.4	87.9	92.4	95.0	81.7	89.3	<u>90.6</u>	94.0	95.7	86.7	91.8	<u>91.6</u>	94.6	95.7	87.2	92.3
APLA	82.4	<u>91.4</u>	93.5	84.5	88.0	88.0	<u>94.0</u>	96.0	88.2	91.6	<u>90.6</u>	95.1	96.5	89.2	92.9	91.7	95.4	96.8	89.5	93.4

off comparison in terms of GPU memory consumption and latency during training across different model sizes in Figure 4. As the model size increases, APLA outperforms all other methods both in terms of predictive performance and costs during training.

B.2. Computational Costs of Adaptation Methods

We analyze the computational costs of adaptation methods by measuring GPU memory footprint and latency during training and inference. Results are shown in Figure 5. During training, APLA is the most efficient method in terms of GPU memory usage and latency and does not add any extra costs during inference. While APLA appears to tune more parameters than other adaptation methods, one should note that parameter count alone does not necessarily reflect the true computational costs. This inconsistency has been previously emphasized by other studies [4, 13]

B.3. Computational Costs of Low-rank Adaptation Methods When Increasing r

In Table 9 in the main text, we investigated the impact of applying other low-rank adaptation methods on W_O , isolating the impact of the low-rank adaptation strategy. Using the same setup, here we analyze their computational costs with respect to the choice of rank r , considering GPU memory and latency during training. As shown in Figure 6, APLA is the only method that only minimally impacts memory and latency during, whereas other methods are affected to a larger extent as r grows (e.g. FACT). Essentially, for any given rank r , APLA outperforms all other low-rank adaptation methods in terms of efficiency, requiring less GPU memory and enabling faster training. This advantage is due

to APLA’s more efficient low-rank strategy and its avoidance of introducing additional trainable parameters. This provides APLA a distinct advantage, allowing the rank to be freely adjusted for optimal results without any extra computational concerns.

B.4. APLA on Increasing Number of ViT Blocks

We investigate the impact of applying APLA to increasing number of ViT blocks, when starting from the first layer and moving towards the last layers (“Bottom → Top”) and the opposite direction (“Top → Bottom”), and present the results in Figure 7. Applying APLA to more blocks monotonically improves performance. As expected, applying APLA to later transformer blocks leads to greater performance improvements than applying it to the early ViT layers.

B.5. The Effect of Choice of r

In APLA, the hyperparameter r is used to specify how many columns of the weight matrix W_O are tuned. In Figure 8, we present the selected values of r for general classification tasks (left), datasets with limited data (middle), and all datasets together (right).

B.6. Feature Visualization

As a last sanity check, we evaluate the quality of learned representations when using APLA and compare them with those obtained from other adaptation methods, similarly to [6, 31, 42]. In Figure 9 we use t-SNE [59] to visualize the final representations derived from the [CLS] token of the last ViT block for various datasets from VTAB. Similar to other adaptation methods, APLA generates well-separated

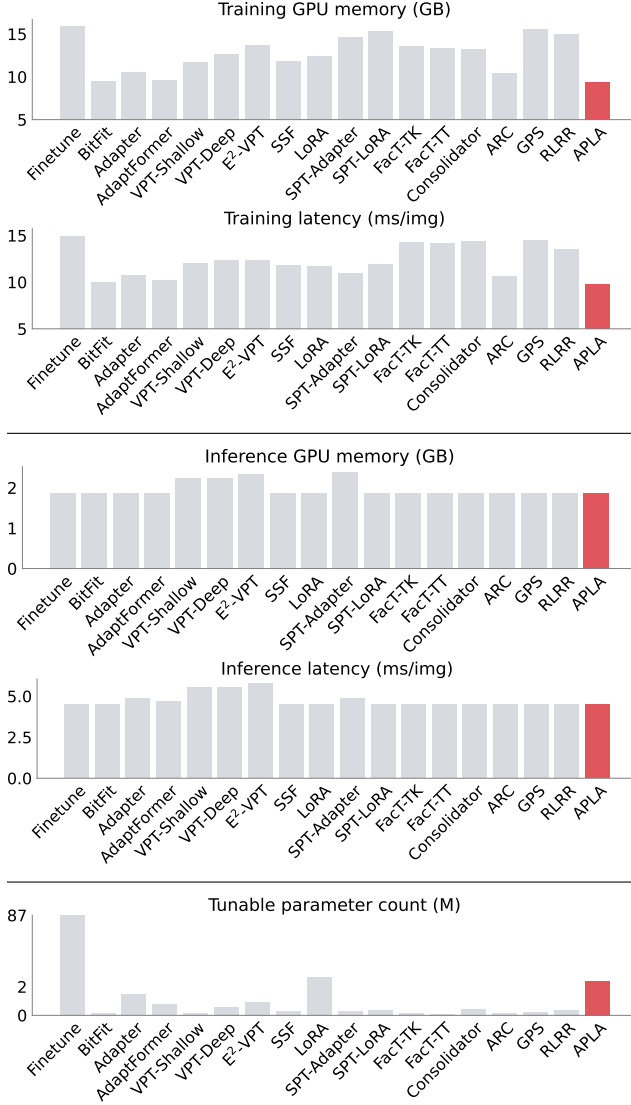


Figure 5. *Computational costs.* We report memory footprint and latency of various adaptation methods during training (top) and inference (middle) for ViT-B with a batch size of 64. Additionally, we provide the number of tunable parameter count for each method (bottom), averaged across all the datasets.

clusters for different classes, with data points from the same class positioned closely together.

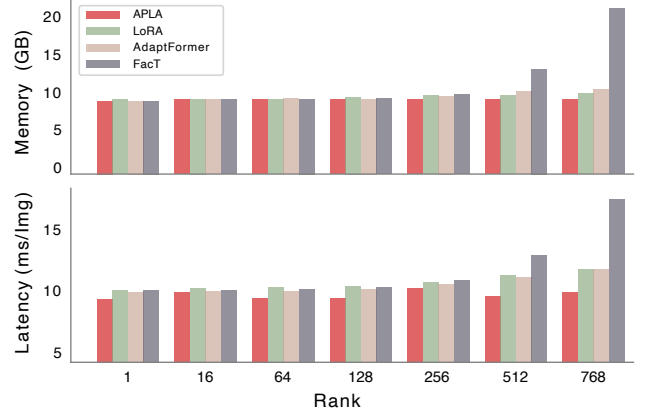


Figure 6. *Computational requirements of different adaptation methods during training for varying r values.* For LoRA and FacT, r denotes the rank, for APLA the number of tuned columns, and for AdaptFormer, the size of the bottleneck dimension.

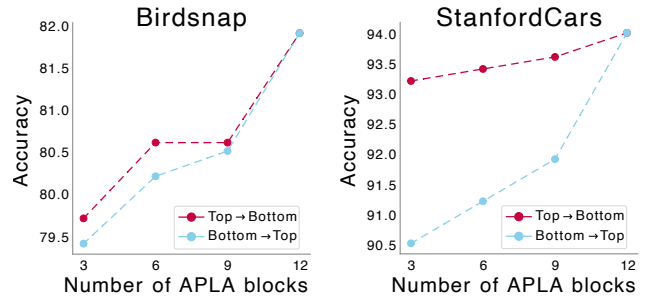


Figure 7. *Classification performance when applying APLA to an increasing number of attention blocks.* “Top-bottom” means applying APLA starting from the last ViT block and moving toward the first layer, while “bottom-top” refers to applying it in the opposite direction.

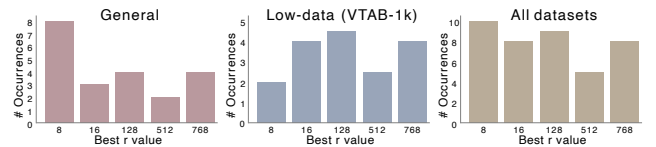


Figure 8. *Selected r values across different datasets.* We report the optimal r values, determined by grid searches, for general classification tasks (left), datasets with limited data (middle), and all datasets (right).

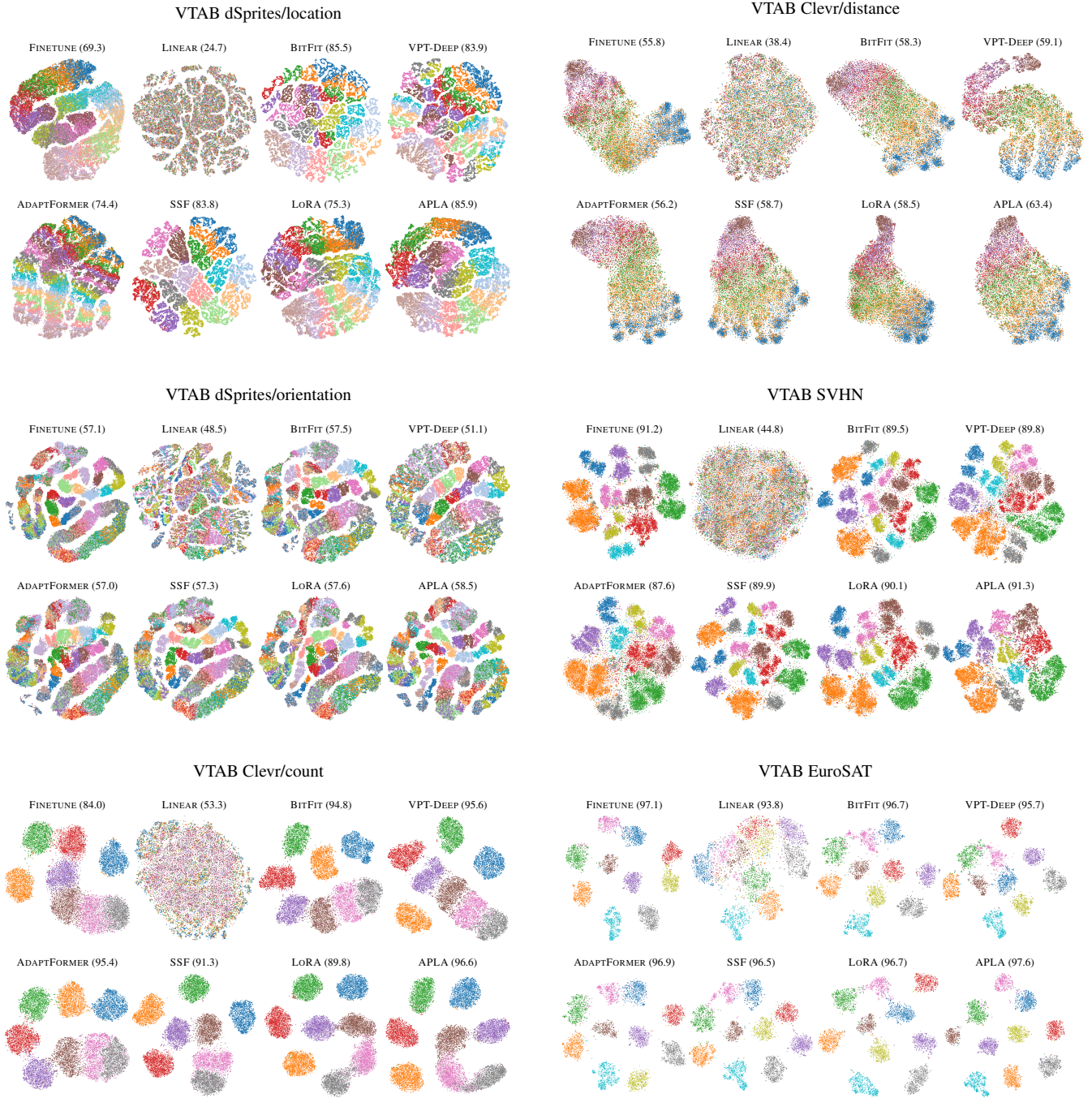


Figure 9. *t-SNE visualizations*. We plot the *t-SNE* visualizations of the output [CLS] embeddings on VTAB using ViT-B models pre-trained with DINOv2. All models have been adapted for each task. The numbers in parentheses indicate each adaptation method’s classification performance for the task.